

0480 0132

(147)
Item 141

CHAPTER P

 **$^{40}\text{Ar}/^{39}\text{Ar}$ STUDIES OF FLUID INCLUSIONS IN
VEIN QUARTZ FROM BATTLE MOUNTAIN,
NEVADA**

By EDWIN H. MCKEE,¹ JAMES E. CONRAD,¹ BRENT D. TURRIN,¹
and TED G. THEODORE¹

ABSTRACT

Fluid inclusions in vein quartz from the Buckingham stockwork molybdenum deposit and from leucogranites north of the Buckingham deposit yield $^{40}\text{Ar}/^{39}\text{Ar}$ isochron ages that agree well with K-Ar and $^{40}\text{Ar}/^{39}\text{Ar}$ radiometric ages of phenocrysts from these rocks. (The Buckingham deposit is Late Cretaceous in age, and the leucogranites north of the Buckingham deposit are late Eocene to early Oligocene in age.) The younger period of igneous activity (late Eocene to early Oligocene) is clearly defined by three isochrons at about 38 Ma. The Late Cretaceous age is recognized by three isochrons, one well defined at 75.5 ± 1.1 Ma, one that is 55.1 ± 3.7 Ma, and one that is 51.2 ± 16.3 Ma. All samples had inherited excess ^{40}Ar in amounts that equal about 30 percent of the total argon. Because of the excess argon, individual age determinations are highly variable and cannot be interpreted—isochores based on several analyses are necessary to yield a meaningful age. Samples with small amounts of potassium proved unusable; sufficient potassium must be present to produce enough radiogenic ^{40}Ar to mask the excess ^{40}Ar .

INTRODUCTION

Igneous activity and associated mineralization in the Battle Mountain district, Nevada (fig. 1), occurred during the Late Cretaceous and again in late Eocene to early

Oligocene time. These age designations are based on many K-Ar and $^{40}\text{Ar}/^{39}\text{Ar}$ age determinations (Theodore and others, 1973; McKee, 1992). The purpose of this study was to determine the radiometric ages of quartz veins from the Cretaceous Buckingham stockwork molybdenum deposit and nearby Eocene and Oligocene quartz veins in this district using single-grain laser-fusion $^{40}\text{Ar}/^{39}\text{Ar}$ methods. The fluid-inclusion-derived ages from this well-dated district are compared with existing K-Ar and $^{40}\text{Ar}/^{39}\text{Ar}$ dates to test the feasibility of obtaining usable geochronology from fluid inclusions. Vein quartz can be dated using argon produced by radioactive decay of potassium-bearing phases in fluid inclusions. All argon from quartz should be derived from fluid inclusions because there is no other site possible for the large K atom in the SiO_2 structure of quartz. Argon is present as a component of paleohydrothermal fluids trapped in fluid inclusions. As the data were gathered, however, it became evident that excess argon is present within the vein quartz. Only by constructing isochrons from a number of individual quartz grains is it possible to evaluate the amount of excess argon present. The ages determined by this technique confirm those derived by K-Ar and $^{40}\text{Ar}/^{39}\text{Ar}$ total fusion and incremental heating of potassium-bearing minerals from the Buckingham deposit (McKee, 1992).

The presence of argon in fluid inclusions in quartz was first demonstrated by Wahler (1956). Subsequently, excess Ar and He in beryl, cordierite, and tourmaline, which were assumed to come from fluid inclusions, was reported by Damon and Kulp (1958). The presence of Ar, Kr, and Xe in gas from gas inclusions in sylvite from the Bereznikovsk mine in Russia was reported by Nesmelova (1959). Excess ^{40}Ar in several quartz and fluorite samples was documented by Rama and others (1965), and they pointed out the difficulties that this presents for

¹U.S. Geological Survey, Mail Stop 901, 345 Middlefield Road, Menlo Park, CA 94025

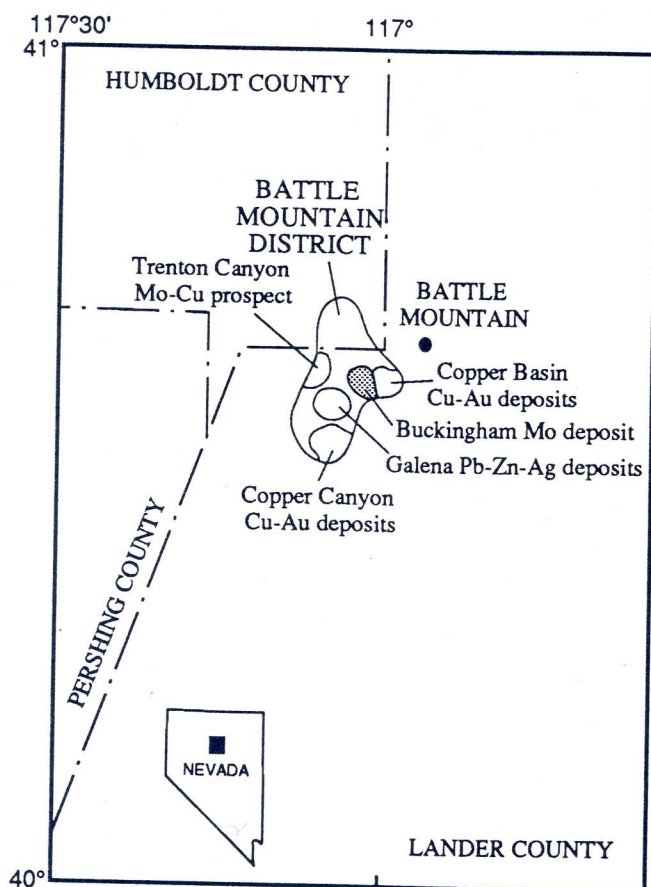


Figure 1. Map of north-central Nevada, showing Battle Mountain district and mineral deposits within it.

K-Ar dating. Little work has been published on K-Ar or $^{40}\text{Ar}/^{39}\text{Ar}$ dating of fluid inclusions since these studies.

Recently, Kelly and others (1986) examined, by incremental heating $^{40}\text{Ar}/^{39}\text{Ar}$ techniques, the Ar isotopes of fluid inclusions in quartz veins associated with granite-hosted tungsten mineralization in southwestern and northern England. In this study, the authors noted that argon in the fluid inclusions is released during incremental heating in amounts that correlate with the potassium and chlorine content of fluid inclusions. The argon in the potassium-correlated component is derived primarily from in situ decay of potassium in solid phases in the inclusions. Argon from the chlorine-correlated component is associated with brines that constitute the liquid phase of the inclusions. Inherited argon from the original magmatic fluid was not noted.

METHODS

Samples 79C103 and 79C104 were irradiated in the U.S. Geological Survey TRIGA reactor (Denver, Colo.)

for a period of 60 h. Irradiation flux was monitored by use of the MMhb-1 hornblende standard, which has an age of 513.9 Ma. Sample handling techniques and corrections for Ca- and K-derived isotopes used in the Menlo Park laboratory are as described by Dalrymple and Lanphere (1971, 1974). Samples 1471-760, 1471-173, 79C77, and 81TT121 were irradiated in the Berkeley TRIGA reactor (University of California, Berkeley) for a period of 10 h. Irradiation flux was monitored by use of standards MMhb-1 (hornblende), GHC 305 (biotite, with an age of 103.76 Ma), and P-207 (muscovite, with an age of 82.1 Ma). Potassium and calcium corrections for the Berkeley TRIGA reactor were determined using optical grade CaF_2 and a laboratory potassium glass.

The $^{40}\text{Ar}/^{39}\text{Ar}$ analyses were conducted at the U.S. Geological Survey, Menlo Park, California, and at the Berkeley Geochronology Center using similar laser-fusion microextraction systems to analyze single grains of vein quartz that were approximately 0.5–1.0 mm in size. An on-line, ultrasensitive mass spectrometer was used for argon analyses.

GEOLOGIC SUMMARY

The Buckingham stockwork molybdenum deposit in north-central Nevada, about 10 km southwest of the town of Battle Mountain (fig. 1), contains one of the largest known resources of molybdenum in the United States. However, under present (1991) economic conditions, the relatively low molybdenum grades of the deposit make it uneconomic. The Buckingham deposit is a calc-alkaline, stockwork-molybdenum-bearing system located on the east flank of the Battle Mountain mining district (fig. 1). The deposit contains an estimated 1,000 million tons of mineralized rock, averaging approximately 0.10 percent molybdenum (as MoS_2). The deposit also contains small amounts of silver, tungsten, copper, and gold (Theodore and others, 1992). Molybdenum mineralization is related to emplacement of a Late Cretaceous composite porphyry system that intruded surrounding Paleozoic rocks and altered much of the country rock to hornfels.

Two periods of plutonism have been recognized in the Battle Mountain area (Theodore and others, 1992). The older period, represented by monzonites at Buckingham and the granodiorite of Trenton Canyon (on the west edge of the mining district and about 9.5 km due west of the Buckingham system), has been dated at about 86 Ma (McKee, 1992) (table 1, fig. 2). The younger period includes at least six Tertiary intrusive bodies in the Buckingham vicinity, ranging in age from 41.1 to 37.3 Ma (Theodore and others, 1973) (table 1, fig. 2).

Table 1. K-Ar and $^{40}\text{Ar}/^{39}\text{Ar}$ ages of Buckingham stockwork system and nearby intrusive rocks.[σ , standard deviation. Modified from McKee (1992)]

Rock type	Mineral dated	Apparent age (Ma $\pm \sigma$)
Samples from the Buckingham stockwork system		
Monzogranite porphyry	Muscovite	61.3 \pm 1.5
Monzogranite porphyry	Muscovite	61.7 \pm 1.5
Monzogranite porphyry	Biotite and chlorite	65.1 \pm 1.6
Monzogranite porphyry	Muscovite	68.6 \pm 1.5
Aplite	Whole rock	70.3 \pm 1.7
Monzogranite porphyry	Muscovite	75.7 \pm 1.6
Monzogranite porphyry	Muscovite	77.4 \pm 1.6
Monzogranite porphyry	Muscovite	85.5 \pm 1.9
Monzogranite porphyry	Biotite	85.7 \pm 0.4 ¹
Monzogranite porphyry	Muscovite	86.1 \pm 2.0
Monzogranite porphyry	Muscovite	88.0 \pm 2.0
Samples of intrusive rocks north and southwest of the Buckingham stockwork system		
Rhyolite	Biotite	37.3 \pm 1.1
Leucotonalite	Hornblende	37.7 \pm 1.4
Monzogranite	Biotite	38.8 \pm 1.1
Monzogranite	Hornblende	39.0 \pm 1.1
Monzogranite	Hornblende	39.3 \pm 1.0
Rhyolite	Biotite	39.1 \pm 1.0
Sample of intrusive rock northeast of and cutting the Buckingham stockwork system		
Granodiorite porphyry	Hornblende	35.4 \pm 1.1

¹ Age from the two greatest release steps from an incremental heating $^{40}\text{Ar}/^{39}\text{Ar}$ experiment.

CRETACEOUS MONZOGRAUNITES OF THE BUCKINGHAM AREA

The age of emplacement of the Buckingham system is based on evaluation of one incremental-heating $^{40}\text{Ar}/^{39}\text{Ar}$ determination and 10 K-Ar age determinations (McKee, 1992) (table 1). The ages range from 88.0 \pm 2.0 to 61.3 \pm 1.5 Ma; four of the K-Ar ages and the major argon release steps of the incremental heating experiment cluster around 86 Ma. This age (86 Ma) is considered to represent the initial time of cooling of the porphyry system.

Eight major intrusive phases identified in the Buckingham system were intruded sequentially from south to north across a distance of several kilometers. The present configuration of the intrusive center is an east-west alignment of two stocks (each a composite of several porphyries) and several outlying intrusive bodies (fig. 2). All eight intrusive phases underwent molybdenum mineralization. The two oldest intrusions form border phases, and the youngest, an outlying intrusion, produced relatively little molybdenum mineralization. The main Buckingham molybdenum deposit, formed by five igneous phases associated with the main part of the two stocks, developed

umbrella-shaped shells of molybdenite mineralization that drape over the stocks (Theodore and others, 1992). Approximately one-half of the Buckingham deposit is hosted in metamorphosed and intensely veined rocks belonging to the Upper Cambrian Harmony Formation. Secondary, partially chloritized biotite is pervasive throughout the Buckingham porphyry and yields a K-Ar age significantly younger (by 10 to 15 percent) than the 86-Ma age that is considered to be the age of initial cooling of the pluton. This younger age is interpreted to result from partial loss of argon from the 86-Ma porphyry (McKee, 1992).

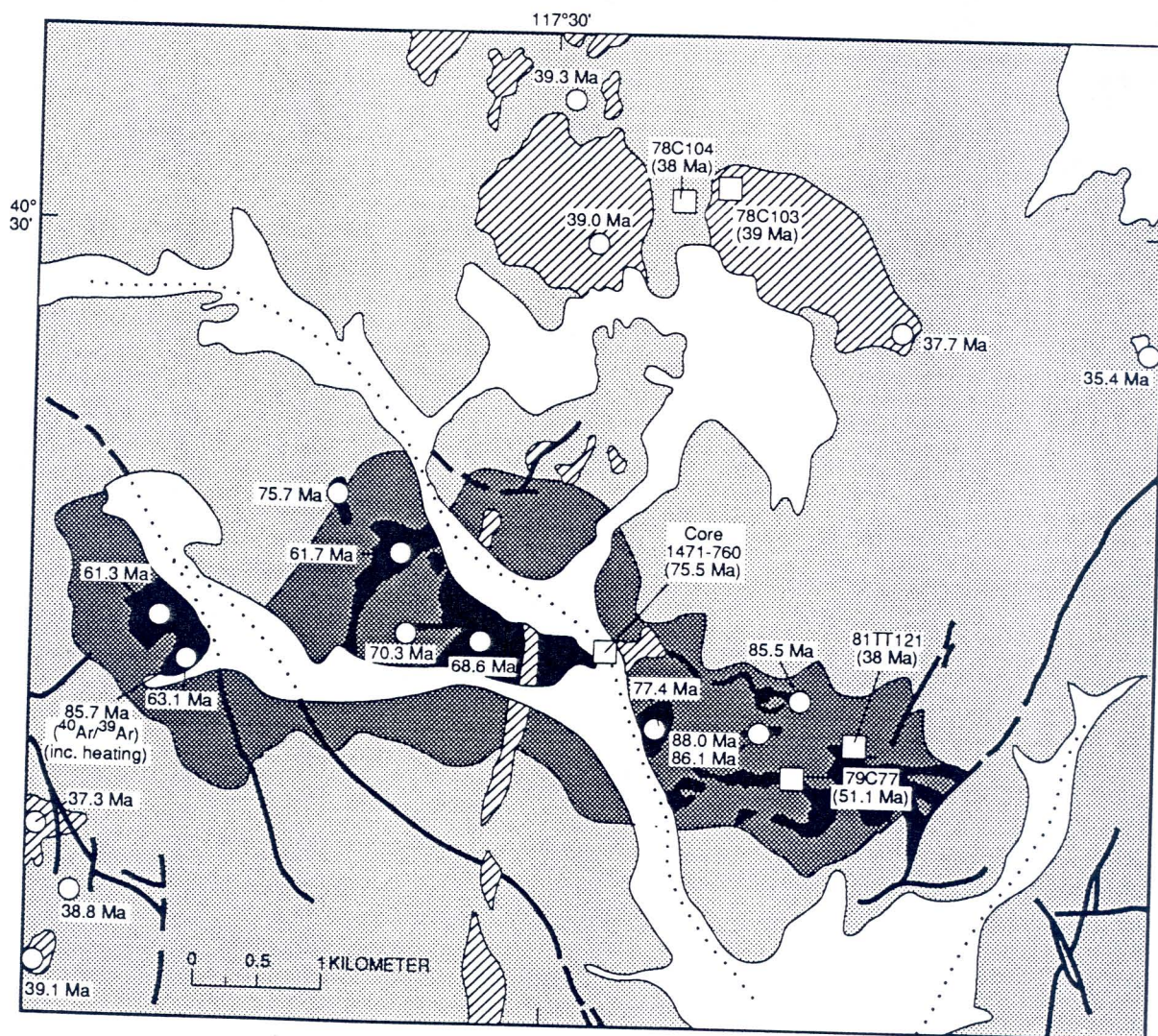
The argon release pattern from the incremental-heating $^{40}\text{Ar}/^{39}\text{Ar}$ experiment support the partial-argon-loss model, indicating a complex thermal history. The secondary thermal event, although not pervasive enough to completely reset the K-Ar clock, is clearly recognized in the release pattern (fig. 3). Heat and hydrothermal activity generated by the late Eocene and early Oligocene igneous events show varying amounts of intensity at different places throughout the Buckingham system. Almost all samples from the western part of the system yield ages that are variably reset, although none of them are completely reset to the approximate 38-Ma age of the younger, nearby plutons.

TERTIARY GRANITIC AND RHYOLITIC INTRUSIVE ROCKS

The six small monzogranite, granodiorite porphyry, and rhyolite stocks and dikes in the vicinity of the Buckingham deposit (fig. 2) yield K-Ar ages on biotite and hornblende of about 38 Ma (table 1). These bodies are mostly satellites of the main Cretaceous monzogranite porphyry of the Buckingham deposit. A system of granodiorite porphyry dikes, dated at about 35 Ma, cut the Buckingham porphyry (table 1, fig. 2). Hydrothermal alteration and mineralization related to late phases of this pervasive middle Tertiary period of igneous activity are recognized south of the Buckingham deposit, at Copper Canyon, and at many other places in the Battle Mountain mining district. The thermal effect of late Eocene and early Oligocene intrusive events manifests itself in the Cretaceous Buckingham system as partially reset K-Ar ages.

STRUCTURE

Deformation of the Buckingham system during the middle Tertiary included significant brittle-type faulting that is manifested primarily along three major, low-angle, normal faults. This Tertiary extensional tectonism progressed from east to west during Oligocene and possibly



EXPLANATION

- Quaternary alluvium
- Tertiary igneous rocks
- Cretaceous Buckingham stockwork system—includes monzogranite (black)
- Paleozoic sedimentary and metasedimentary rocks
- 38.8 Ma
K-Ar or $^{40}\text{Ar}/^{39}\text{Ar}$ sample locality—showing age determinations from McKee (1992)
- 75.5 Ma
 $^{40}\text{Ar}/^{39}\text{Ar}$ quartz vein, fluid-inclusion sample site and age
- Fault—dotted where concealed

Figure 2. Geologic map of the Buckingham stockwork molybdenum deposit and surrounding area. Sample sites for this report are represented by squares; K-Ar sample sites and one $^{40}\text{Ar}/^{39}\text{Ar}$ incremental-heating-age sample site represented by circles.

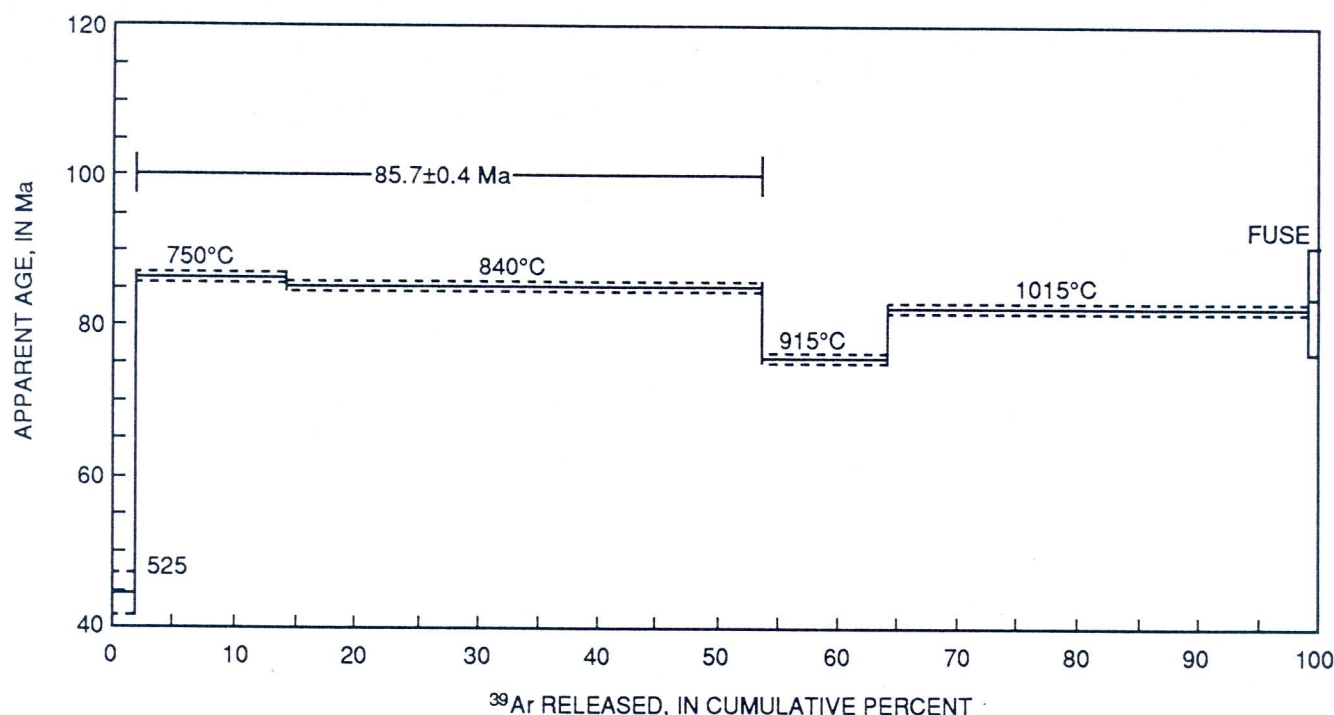


Figure 3. $^{40}\text{Ar}/^{39}\text{Ar}$ age spectra for a biotite from the Buckingham stockwork system (monzogranite porphyry). The six heating steps (and thus temperature in $^{\circ}\text{C}$) are shown as horizontal bars. This release pattern is similar to patterns produced from minerals with disturbed thermal histories. The most likely age calculated using the two oldest steps (which produced more than 50 percent of the Ar) is 85.7 ± 0.4 Ma (from McKee, 1992).

Miocene time (Theodore and others, 1992). Imbricate, down-to-the-east, listric-normal faults merge into a single, flat-lying dislocation east of the Buckingham porphyry system. In addition, major reverse dislocations in the hanging wall of the major fault probably reflect development of antithetic reverse faults in the toe region of a rigid-body glide block (Theodore and others, 1992).

FLUID INCLUSIONS

Hydrothermal fluids in the Buckingham system show complex histories that reflect successive influxes of fluids from newly injected magma into loci of earlier emplaced igneous phases (Theodore and others, 1992). In distal parts of the system, fluid inclusions in andradite-diopside suggest temperatures of about 300°C at extremely low mole fractions of CO_2 . In proximal parts of the system, where the bulk of the quartz stockworks and molybdenite was deposited, fluids were relatively low-density, low-salinity NaCl brines that included variable amounts of CO_2 . These early-stage fluids established an ascending plume of fluid that was considerably less saline than fluids associated with most porphyry copper systems in the southwestern United States. The magmas at the Buckingham deposit did not evolve large volumes of very dense,

NaCl-rich fluids. High in the system, very sparse halite-bearing fluid inclusions formed through condensation from an earlier, higher temperature saline fluid. In the western part of the system, the high-temperature and high-saline halite-bearing fluid inclusions, having salinities as much as 65 weight percent NaCl equivalent and homogenization temperatures as high as 500°C , probably reflect ponded magmatic fluids from a deep source. Overall distribution of veins associated with such fluids appears to be restricted. Although a fluid-immiscibility model is probably applicable to some porphyry molybdenum systems where the exposed parts of the system are above a buried concentration of molybdenum, the geometry of the molybdenite-enriched shells and their proximity to the igneous source at the Buckingham deposit argue against this model. These shells are tightly constrained to the flanks and apical parts of the two mineralized stocks, and the shells show a genetic relationship to a quartz-potassium feldspar porphyry phase in the core of the stocks. Furthermore, an approximately 1-km-long composite vertical section through the Buckingham system is available for study in the three tectonically offset blocks, and nowhere is there widespread occurrence of hypersaline fluids. The bulk of the moderately saline, H_2O -NaCl- CO_2 mineralizing fluids associated with this deposit is related to quartz-potassium feldspar porphyry and slightly deeper

Table 2. Temperature and salinity data for vein quartz samples used for fluid inclusion studies.[Locations of samples used for $^{40}\text{Ar}/^{39}\text{Ar}$ analyses shown on fig. 2; salinity ranges given in weight percent NaCl equivalent; --, not determined]

Sample no.	Host rock ¹	Homogenization temperature range (°C) ²	Fluid-inclusion types ³	Salinity range ²	Comments
Outcrop samples					
79C77	Km	--	I, II, IV	--	Quartz veins on Vail Ridge associated with Buckingham system.
81TT121	Km	229–324	I, IV	0–11.6	Quartz veins in upper copper-rich part of Buckingham system.
78C103	Ch	--	I, II, III, IV	--	Quartz stockworks near Tertiary leucogranite.
78C104	Ch	--	I, II, III	--	Quartz stockworks in pendant within Tertiary leucogranite.
87TT215A	Chg	175–550	I, II, III	1.3–48.5	Quartz stockworks near Tertiary leucogranite.
87TT215B	Chg	250–600	I, II, III	3.0–62	Quartz stockworks near Tertiary leucogranite.
Samples from diamond drill core					
1453-259.8	Km	261–328	I, II	7.8–10.8	Drill hole collared in east stock of Buckingham system.
1471-173	Km	--	I, II, IV	--	Drill hole collared in Vail block part of Buckingham system.
1471-760	Km	292–345	I, II, IV	--	Drill hole collared in Vail block part of Buckingham system.

¹ Km, Cretaceous monzogranite; Ch, Upper Cambrian Harmony Formation hornfels; Chg, garnet skarn developed in Upper Cambrian Harmony Formation and related genetically to 38-Ma leucogranite (see text).² From Theodore and others (1992); Theodore and Hammarstrom (1991).³ At 22 ± 2°C: I, low vapor volume, mostly liquid H₂O; II, high vapor volume, mostly liquid H₂O; III, halite bearing, commonly with other daughter minerals; IV, mostly CO₂ vapor with some liquid CO₂, mostly H₂O liquid (see text).

equivalent igneous phases. A summary of fluid-inclusion types recognized in the Buckingham stockwork system is shown in figure 4, and temperature and salinity data for the fluid inclusions is in table 2.

In this study, $^{40}\text{Ar}/^{39}\text{Ar}$ values from fluid inclusions were measured on 29 approximately 1-mm grains from four samples of vein quartz from three localities (including a drill core) that are associated genetically with the Cretaceous Buckingham stockwork molybdenum system (table 2). These four samples were not found to include any of the type-III fluid inclusions (fig. 4), i.e., the daughter-mineral-bearing variety; nonetheless, it is possible that some sylvite and (or) other potassium-bearing minerals may have been present in the quartz fragments selected for argon analysis because other samples from the system contain some sylvite-bearing fluid inclusions. In addition, $^{40}\text{Ar}/^{39}\text{Ar}$ measurements were made from fragments of vein quartz associated with the 38-Ma leucogranite. These samples are from two localities (fig. 2): one vein (78C104) intrudes the Harmony Formation about 500 m west of a relatively large body of leucogranite, and the other (78C103) intrudes the leucogranite. In contrast with the samples from the Buckingham system, the vein quartz

associated with the 38-Ma leucogranite contains abundant concentrations of type III, daughter-mineral-bearing fluid inclusions (fig. 4). Many of these type-III fluid inclusions contain sylvite (Theodore and others, 1992; Theodore and Hammarstrom, 1991).

$^{40}\text{Ar}/^{39}\text{Ar}$ ANALYSIS OF FLUID INCLUSIONS

$^{40}\text{Ar}/^{39}\text{Ar}$ analyses on fluid inclusions in quartz from the Battle Mountain district show a wide range of ages. Apparent ages of individual quartz grains are from about 40 Ma to about 1,747 Ma (table 3, no. 101-6). These ages are interpreted to represent the product of inherited excess ^{40}Ar from magmatic sources trapped in fluid inclusions plus the component of radiogenic ^{40}Ar derived from the decay of potassium-bearing fluids and solids trapped in fluid inclusions. This interpretation is supported by the association of the younger ages with a relatively high release of ^{39}Ar and a corresponding increase in age with lower ^{39}Ar releases. Fluid inclusions containing essentially no potassium

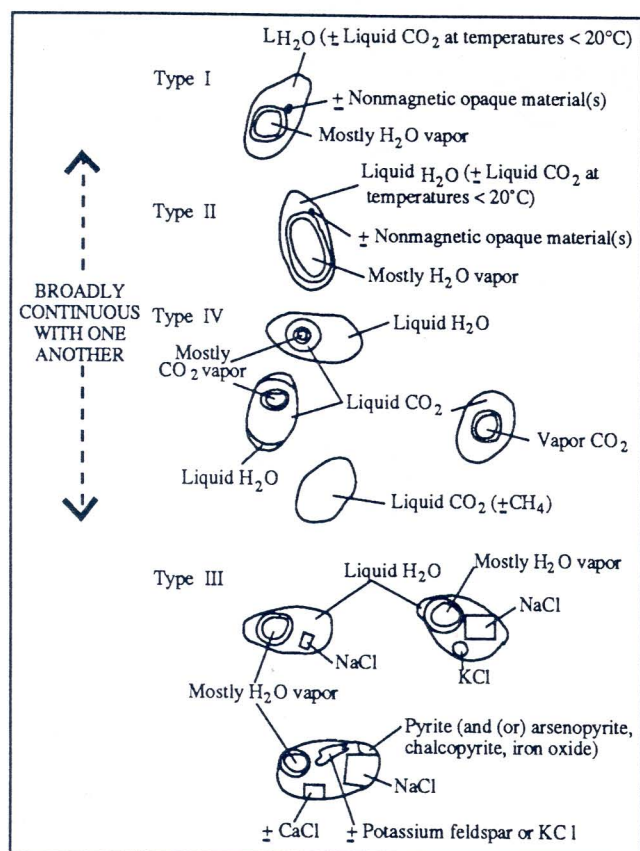


Figure 4. Types of fluid inclusions recognized in the Buckingham stockwork molybdenum system (modified from Theodore and others, 1992).

therefore give anomalously old $^{40}\text{Ar}/^{39}\text{Ar}$ ages, whereas fluid inclusions with high potassium content can produce enough radiogenic ^{40}Ar to almost entirely mask the presence of the excess ^{40}Ar component.

The ages determined from individual grains of samples of the Buckingham quartz stockwork are extremely variable and give no indication of the age of the fluid inclusions, assuming that they are Cretaceous as is indicated by previous studies (McKee, 1992). As noted, samples with very little potassium give anomalously old ages with analytical precision values as great or greater than the age. For instance, two grains from sample 79C77 (fig. 2) that contain very little potassium yield ages of $1,748 \pm 1,306$ Ma and $1,314 \pm 660$ Ma (table 3). Grains with greater amounts of potassium, however, provide points on a $^{40}\text{Ar}/^{36}\text{Ar}$ versus $^{39}\text{Ar}/^{36}\text{Ar}$ diagram from which an isochron can be drawn that defines the age of the fluid inclusions in the total sample (broken to produce the individual grains). The isochron also gives a measure of the amount of excess argon in the sample (intercept on the ordinate with a value greater than 295.5). Samples 1471-760, 1471-173, and 79C77 define isochrons (figs. 5, 6, and 7) that are interpreted to be between about 60 and 76 Ma.

This is similar to the range of K-Ar and $^{40}\text{Ar}/^{39}\text{Ar}$ incremental heating ages from biotite, muscovite, and whole-rock samples from the Buckingham stockwork system (McKee, 1992) (table 1).

Sample 81TT121, which was expected to give a Late Cretaceous age (60 to 76 Ma), yielded a well-constrained isochron of 37.2 ± 5.3 Ma (fig. 8). This late Eocene or early Oligocene age is the same as many of the small igneous bodies in the Battle Mountain district (McKee, 1992) (table 1). We assume that this age represents either almost complete replacement of the bulk of the fluid in older Cretaceous quartz by middle Tertiary fluid or that the quartz vein is a late Eocene to early Oligocene vein that is not recognized as such in the Cretaceous Buckingham stockwork system. The former alternative is more likely. The fluid-inclusion population hosted by the quartz vein in sample 81TT121 differs in many aspects from that near the fringes of the system. Firstly, the overwhelming bulk of the fluid inclusions, mostly type I (fig. 4), are secondary relative to vein quartz, and they are concentrated in dense swarms along annealed microcracks oriented at high angles to the walls of the veins (Theodore and others, 1992). These fluid inclusions must have been repeatedly trapped mostly during circulation of fluids associated with a widespread and locally intense, late-stage, argillic overprint that has affected these rocks. Nonetheless, almost all these veins still show relict potassic-alteration assemblages along their selvages that suggest that initial emplacement of veins occurred during potassic-alteration stages of the system. Although the overwhelming bulk of the fluid inclusions in the veined porphyry are the type I variety, these veins also seem to show a slightly increased abundance of halite-bearing, type-III-variety fluid inclusions relative to veins at the fringes of the system. Furthermore, liquid-vapor homogenization tests of fluid inclusions from these quartz veins in the monzogranite porphyry yield a plot significantly different from that derived from quartz veins that are minimally affected by postpotassic alteration. This difference results in a 100°C difference between medians for the two temperature-of-homogenization plots (380°C for the potassic-alteration assemblage, compared with 280°C for veins showing intense development of the intermediate argillic overprint). Thus, the apparent preferred concentration of fluid inclusions that homogenized to vapor at the high-temperature end of the distribution plot for samples of veined porphyry in the general area of sample 81TT121 suggests that these high-temperature fluid inclusions may be largely relict from early potassic stages (Theodore and others, 1992). In addition, circulation of fluids during the middle Tertiary in this part of the Cretaceous porphyry system is probably related to small bodies of Tertiary intrusive rocks not shown on figure 2.

Of the samples that produced Cretaceous isochron ages, number 1471-760 (760 ft depth in core hole shown

Table 3. Summary of single-grain laser-fusion $^{40}\text{Ar}/^{39}\text{Ar}$ analyses of quartz from the Battle Mountain district.[Ages calculated using $\lambda_{\text{e}}=0.581 \times 10^{-10} \text{ yr}^{-1}$, $\lambda_{\text{p}}=4.962 \times 10^{-10} \text{ yr}^{-1}$, $^{40}\text{K}/\text{K}_{\text{total}}=1.167 \times 10^{-4}$ moles/mole. Errors are estimates of the standard deviation (σ) of analytical precision]

Sample no.	Experiment no.	$^{40}\text{Ar}/^{39}\text{Ar}$	$^{38}\text{Ar}/^{39}\text{Ar}$	$^{37}\text{Ar}/^{39}\text{Ar}$	$^{36}\text{Ar}/^{39}\text{Ar}$	^{40}Ar rad ($\times 10^{-14}$ moles)	^{40}Ar rad/ ^{39}Ar	^{40}Ar rad (percent)	Apparent age ($\pm 1\sigma$) (Ma)
Quartz veins from the Buckingham stockwork system									
1471-760 ¹ (fig. 5)	100-1	143.36	0.17742	1.0008	0.29231	3.1992	57.085	39.81	268.4 \pm 46.2
	100-2	542.86	0.65356	0.93087	1.6314	6.8823	60.881	11.21	284.9 \pm 18.1
	100-3	17.762	0.021477	0.050199	0.008106	50.853	15.363	86.49	76.24 \pm 0.59
	100-4	184.32	0.54344	0.54672	0.19733	0.78051	126.07	68.39	547.1 \pm 113.0
	100-5	17.213	0.019658	0.000707	0.005415	21.353	15.604	90.65	77.42 \pm 0.73
	100-6	874.42	1.6889	0.48291	1.4799	0.87615	437.22	49.99	1,445 \pm 1,022
	100-7	1183.2	1.5772	0.38085	2.7903	0.91207	358.75	30.32	1,257 \pm 1,343
1471-173 ¹ (fig. 6)	114-1	175.69	0.27240	0.025152	0.31226	4.5563	83.411	47.48	379.9 \pm 60.0
	114-2	29.938	0.047228	0.35130	0.03736	27.980	18.922	63.20	93.46 \pm 2.77
	114-3	33.953	0.057976	0.38035	0.05322	9.6808	18.253	53.75	90.23 \pm 6.63
	114-4	183.46	0.46293	5.2656	0.21180	1.5298	121.52	66.14	530.0 \pm 312.0
79C77 ¹ (fig. 7)	101-1	168.64	0.28784	0.058985	0.36945	12.585	59.465	35.26	278.8 \pm 28.7
	101-2	470.22	0.83678	0.29027	1.1120	19.681	141.64	30.12	604.4 \pm 65.0
	101-3	167.31	0.39749	0.022914	0.23509	2.7926	97.837	58.47	438.2 \pm 75.9
	101-4	1077.0	3.5915	0.19807	2.3541	1.8709	381.39	35.41	1,314 \pm 659
	101-5	22.366	0.024696	0.003383	0.02698	19.424	14.387	64.32	71.50 \pm 1.92
	101-6	1272.3	3.4560	0.32611	2.3367	1.7346	581.86	45.73	1,747 \pm 1,306
81TT121 ¹ (fig. 8)	99-1	11.777	0.021847	0.012340	0.012292	25.827	8.1376	69.10	40.79 \pm 5.57
	99-3	21.739	0.025867	0.000779	0.036843	14.269	10.844	49.88	54.15 \pm 2.42
	99-4	17.261	0.024701	0.003130	0.010519	54.165	14.145	81.94	70.31 \pm 0.89
	99-5	21.742	0.013739	0.000925	0.026141	0.97164	14.009	64.43	69.65 \pm 22.58
	99-6	238.79	1.0214	0.019467	0.55847	0.36695	73.750	30.89	339.8 \pm 276.8
	99-7	44.022	0.11787	0.001111	0.091029	1.4932	17.115	38.88	84.74 \pm 16.84
	99-8	321.18	1.3810	1.1708	0.62517	0.89309	136.58	42.51	586.0 \pm 287.1
	99-9	16.615	0.021366	0.000136	0.020051	7.6325	10.682	64.29	53.35 \pm 2.24
Quartz veins associated with late Eocene to early Oligocene igneous event									
79C103 ² (fig. 9)	89Z0245	5.0156	0.12399	0.22852	0.0031478	9.4073	4.0745	81.22	45.51 \pm 0.28
	89Z0246	8.5362	0.38236	0.067216	0.011091	1.4048	5.2356	61.33	58.27 \pm 0.48
	89Z0247	10.825	0.47548	1.5676	0.015082	0.67411	6.4626	59.64	71.66 \pm 0.85
	89Z0248	7.5420	0.36763	1.1612	0.010515	0.70169	4.4961	59.57	50.15 \pm 0.58
	89Z0249	5.1823	0.16034	1.2324	0.004525	1.0897	3.9112	75.41	43.71 \pm 0.38
	89Z0250	3.8967	0.037980	0.35426	0.0011497	2.8827	3.5556	91.22	39.78 \pm 0.25
79C104 ³ (fig. 10)	89Z0240	4.6007	0.20468	0.008856	0.0028211	7.4874	3.7393	81.27	41.68 \pm 0.25
	89Z0242	8.3961	1.5301	0.029108	0.012850	0.49378	4.5726	54.46	50.83 \pm 0.76
	89Z0243	7.2386	0.7508	2.1875	0.010203	0.41811	4.3639	60.20	48.54 \pm 0.82
	89Z0244	3.9638	0.075151	0.055961	0.0013574	10.673	3.5385	89.27	39.46 \pm 0.24
	89Z0251	3.7181	0.031822	0.50783	0.0005269	0.47926	3.5728	96.06	39.84 \pm 0.59
	89Z0252	5.2010	0.54699	0.31335	0.0038603	0.23390	4.0559	77.97	45.16 \pm 1.27

1 Reactor corrections: $^{40}\text{ArK}/^{39}\text{ArK}=0.0086$, $^{39}\text{ArCa}/^{37}\text{ArCa}=0.0003$, and $^{36}\text{ArCa}/^{37}\text{ArCa}=0.0003$. $J=0.00281$.2 Reactor corrections: $^{40}\text{ArK}/^{39}\text{ArK}=0.0285$, $^{39}\text{ArCa}/^{37}\text{ArCa}=0.000671$, and $^{36}\text{ArCa}/^{37}\text{ArCa}=0.000251$. $J=0.00627$.3 Reactor corrections: $^{40}\text{ArK}/^{39}\text{ArK}=0.0285$, $^{39}\text{ArCa}/^{37}\text{ArCa}=0.000671$, and $^{36}\text{ArCa}/^{37}\text{ArCa}=0.000251$. $J=0.00625$.

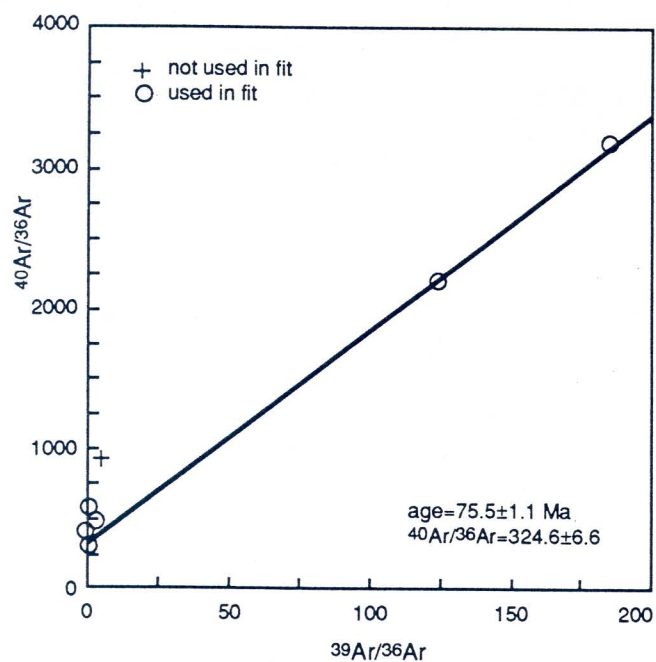


Figure 5. $^{40}\text{Ar}/^{36}\text{Ar}$ versus $^{39}\text{Ar}/^{36}\text{Ar}$ diagram with isochron plot for sample 1471-760. Isochron age is 75.5 ± 1.1 Ma.

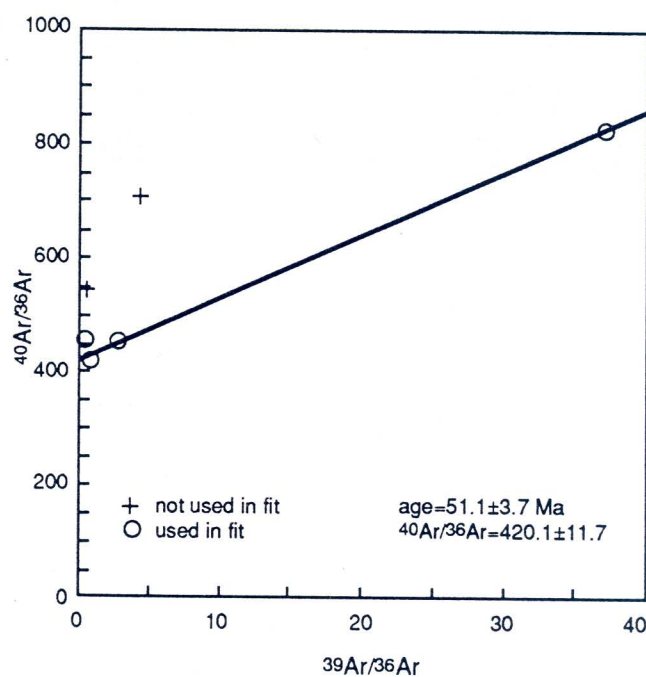


Figure 7. $^{40}\text{Ar}/^{36}\text{Ar}$ versus $^{39}\text{Ar}/^{36}\text{Ar}$ diagram with isochron plot for sample 79C77. Isochron age is 55.1 ± 3.7 Ma.

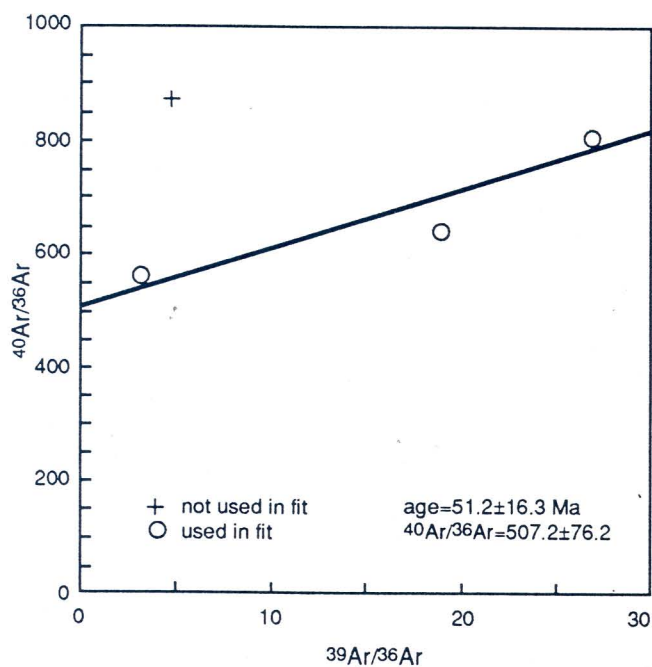


Figure 6. $^{40}\text{Ar}/^{36}\text{Ar}$ versus $^{39}\text{Ar}/^{36}\text{Ar}$ diagram with isochron plot for sample 1471-173. Isochron age is 51.2 ± 16.3 Ma.

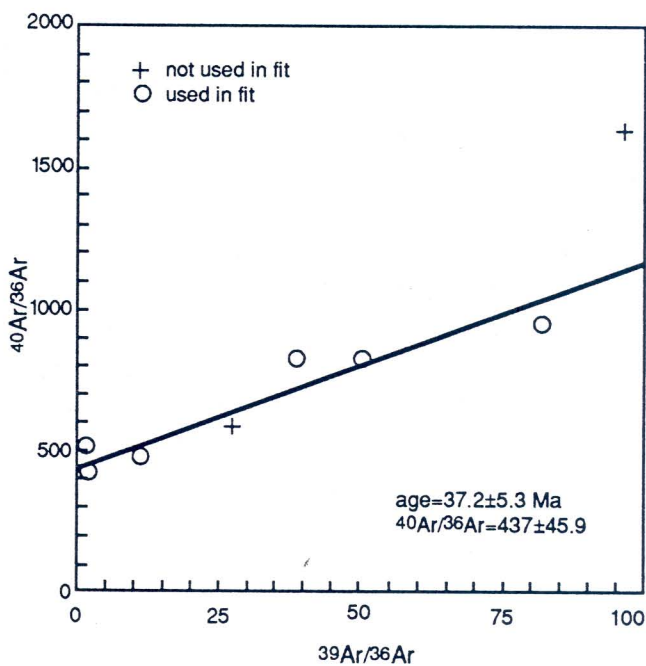


Figure 8. $^{40}\text{Ar}/^{36}\text{Ar}$ versus $^{39}\text{Ar}/^{36}\text{Ar}$ diagram with isochron plot for sample 81TT121. Isochron age is 37.2 ± 5.3 Ma.

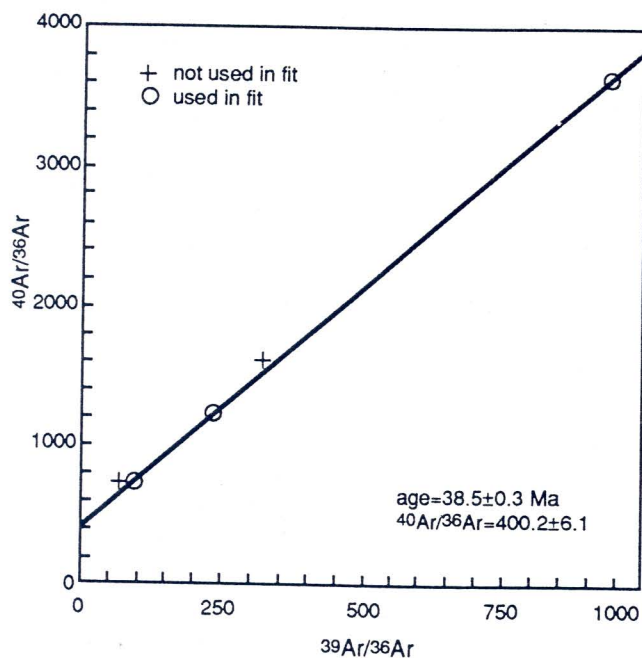


Figure 9. $^{40}\text{Ar}/^{36}\text{Ar}$ versus $^{39}\text{Ar}/^{36}\text{Ar}$ diagram with isochron plot for sample 78C103. Isochron age is 38.5 ± 0.3 Ma.

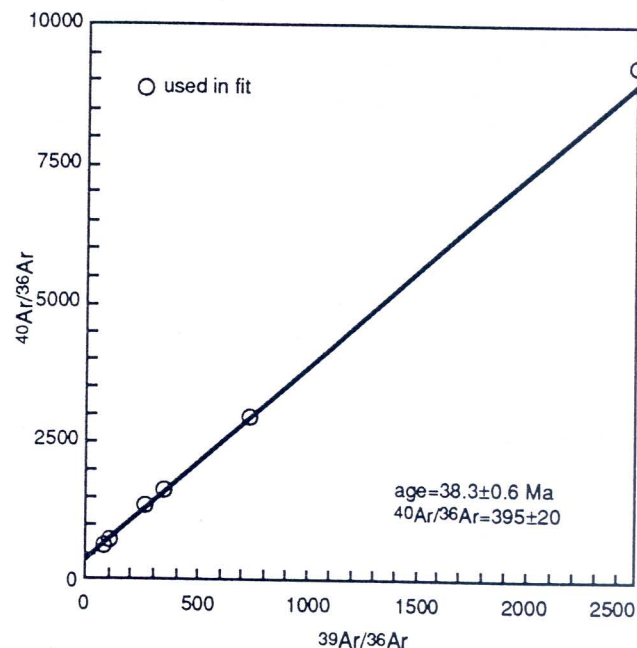


Figure 10. $^{40}\text{Ar}/^{36}\text{Ar}$ versus $^{39}\text{Ar}/^{36}\text{Ar}$ diagram with isochron plot for sample 78C104. Isochron age is 38.3 ± 0.6 Ma.

on fig. 2) gives the best data for drawing an isochron because two analyzed grains had relatively large amounts of potassium (fig. 5). The influence on the isochron by samples with a high value of $^{39}\text{Ar}/^{36}\text{Ar}$ (an indication of the amount of potassium) is a significant factor because the points plot far from the ordinate on the $^{40}\text{Ar}/^{36}\text{Ar}$ versus $^{39}\text{Ar}/^{36}\text{Ar}$ diagram and have relatively more leverage in drawing the best line fit between the plotted points. Six grains define an isochron that is 75.1 ± 1.1 Ma (fig. 5).

A second sample from the drill hole, 1471-173, also yields an isochron that can be interpreted as Late Cretaceous in age (fig. 6). It is much less well constrained, however, and has a much larger uncertainty due to the small amount of potassium in the six grains analyzed. The isochron age of 51.2 ± 16.3 Ma, based on three points, is of little value in determining the age of the quartz fluid inclusions.

Sample 79C77 presented the same problems as sample 1471-173 (see above). Because of very small amounts of potassium and consequently small amounts of ^{39}Ar , the analysis is heavily biased by the excess ^{40}Ar in the fluid of the inclusion. The isochron drawn through four points defines an age of 55.1 ± 3.7 Ma (fig. 7). The slope of the line is strongly influenced by one analysis with the highest $^{40}\text{Ar}/^{39}\text{Ar}$ value (101-5, table 3); the other three analyses cluster near the ordinate and near the 425 ratio, indicating about 30 percent excess argon.

Two samples (78C103 and 78C104, fig. 2) of vein quartz associated with a 38-Ma leucogranite north of the

Buckingham quartz stockwork system produce well-defined isochron ages of 38.5 ± 0.3 Ma and 38.3 ± 0.6 Ma, respectively (figs. 9 and 10). The leucogranite bodies have K-Ar ages on hornblende and biotite of 37.7 ± 1.4 Ma, 38.8 ± 1.1 Ma, and 39.0 ± 1.1 Ma (table 1); this is identical to the fluid-inclusion ages. The trapping of fluid in the quartz must have taken place at the time of cooling of these igneous bodies, and there has been no subsequent modification of the igneous system.

A summary $^{40}\text{Ar}/^{36}\text{Ar}$ versus $^{39}\text{Ar}/^{36}\text{Ar}$ diagram (fig. 11) shows the data points from all the analyses used from the four samples of quartz from the Buckingham quartz stockwork. The age is shown above or below each line. This figure emphasizes the fact that samples with low potassium (and, hence, a low $^{39}\text{Ar}/^{36}\text{Ar}$ ratio) cluster near the ordinate and limit the construction of an isochron if grains that have a higher potassium content are not available. Ideally, a wide variation of potassium content would produce the best isochrons. Samples 78C103 and 78C104 (figs. 9 and 10) are examples in which isochrons are controlled by a wide spread of $^{39}\text{Ar}/^{36}\text{Ar}$ values. They are not plotted on figure 11 because they have points an order of magnitude higher on the $^{39}\text{Ar}/^{36}\text{Ar}$ axis than the other samples.

CONCLUSIONS

$^{40}\text{Ar}/^{39}\text{Ar}$ dating of fluid inclusions in igneous minerals has promise as a means of dating the fluid and, hence,

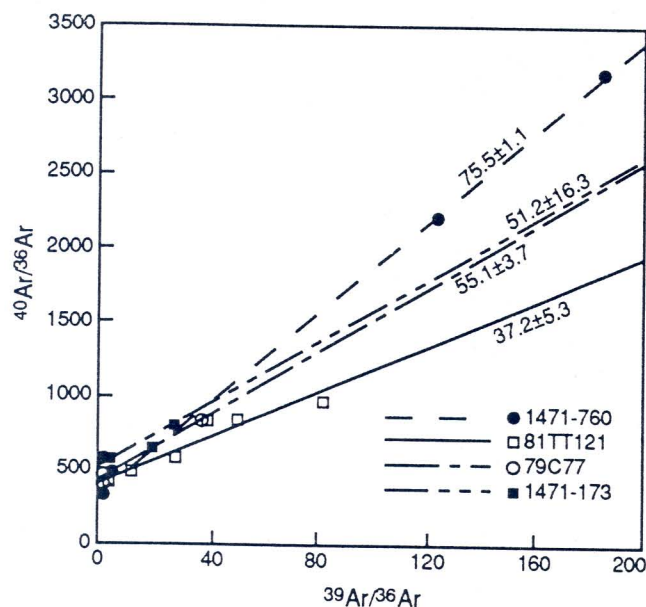


Figure 11. $^{40}\text{Ar}/^{36}\text{Ar}$ versus $^{39}\text{Ar}/^{36}\text{Ar}$ diagram with isochron plots from all Buckingham stockwork samples from the Battle Mountain district.

the age of mineralization (assuming that the two are related and nearly synchronous). Several limiting factors are apparent from the quartz samples from the Battle Mountain mining district, Nevada.

1. Excess inherited ^{40}Ar may be present, and should be expected, in the trapped fluid. Because of this, a number of analyses are needed to provide points on a $^{40}\text{Ar}/^{36}\text{Ar}$ versus $^{39}\text{Ar}/^{36}\text{Ar}$ diagram from which an isochron can be drawn. The slope of the isochron gives the age, and the intercept on the ordinate ($^{40}\text{Ar}/^{36}\text{Ar}$ axis) indicates the amount of excess argon (if the value is above 295.5 or the $^{40}\text{Ar}/^{36}\text{Ar}$ ratio of air).
2. Samples with small amounts of potassium that yield proportionally small amounts of ^{39}Ar on irradiation are difficult to analyze with good precision. These samples produce points on a $^{40}\text{Ar}/^{36}\text{Ar}$ versus $^{39}\text{Ar}/^{36}\text{Ar}$ diagram that cluster near the $^{40}\text{Ar}/^{36}\text{Ar}$ axis and are of little value in describing an isochron. Samples containing small amounts of potassium proved nearly unusable in this study.
3. Areas with several periods of igneous activity, such as Battle Mountain (Late Cretaceous and late Eocene to early Oligocene), probably produce several populations of fluid inclusions. At Battle Mountain, the youngest period of igneous activity (late Eocene to

early Oligocene) proved datable with reasonable confidence. The Late Cretaceous event was evident but obscure. The mechanism for partial argon loss from fluid inclusions and for multiple periods of fluid entrapment in minerals is poorly understood but has a great effect on dating of mixed populations of fluid inclusions by the $^{40}\text{Ar}/^{39}\text{Ar}$ technique.

REFERENCES CITED

- Dalrymple, G. B., and Lanphere, M.A., 1971, $^{40}\text{Ar}/^{39}\text{Ar}$ technique of K-Ar dating: A comparison with the conventional technique: *Earth and Planetary Science Letters*, v. 12, p. 300-308.
- , 1974, $^{40}\text{Ar}/^{39}\text{Ar}$ age spectra of some undisturbed terrestrial samples: *Geochimica et Cosmochimica Acta*, v. 38, p. 715-738.
- Damon, P.E., and Kulp, J.L., 1958, Excess helium and argon in beryl and other minerals: *American Mineralogist*, v. 43, p. 433-459.
- Kelley, S., Turner, G., Butterfield, A.W., and Shepherd, T.J., 1986, The source and significance of argon isotopes in fluid inclusions from areas of mineralization: *Earth and Planetary Science Letters*, v. 79, p. 303-318.
- McKee, E.H., 1992, Potassium-argon and $^{40}\text{Ar}/^{39}\text{Ar}$ geochronology of selected plutons in the Buckingham area, in Theodore, T.G. and others, 1992, *Geology of the Buckingham Stockwork Molybdenum Deposit and Surrounding Area*, Lander County, Nevada: U.S. Geological Survey Professional Paper 798-D, p. D36-D98.
- Nesmelova, Z.N., 1959, Gases in potassium salts of the Bereznikovsk mine: *Trudy Vsesoyuznogo Nauchno-issledovatel'skogo Instituta Galurgii*, n o. 35, p. 206-243.
- Rama, S.N.I., Hart, S.R., and Roedder, Edwin, 1965, Excess radiogenic argon in fluid inclusions: *Journal of Geophysical Research*, v. 70, p. 509-511.
- Theodore, T.G., Silberman, M.L., and Blake, D.W., 1973, Geochemistry and potassium-argon ages of plutonic rocks in the Battle Mountain mining district, Lander County, Nevada: U.S. Geological Survey Professional Paper 798-A, 24 p.
- Theodore, T.G., and Hammarstrom, J.M., 1991, Petrochemistry and fluid-inclusion study of skarns from the northern Battle Mountain mining district, Nevada, in Aksyuk, A.M., ed., *Skarns—Their Genesis and Metallogeny*: Athens, Theophrastus Publications, S.A., p. 497-554.
- Theodore, T.G., Blake, D.W., Loucks, T.A., and Johnson, C.A., 1992, *Geology of the Buckingham stockwork molybdenum deposit and surrounding area*, Lander County, Nevada: U.S. Geological Survey Professional Paper 798-D, 318 p.
- Wahler, William, 1956, Über die in Kristallen eingeschlossenen Flüssigkeiten und Gase: *Geochimica et Cosmochimica Acta*, v. 9, p. 105-135.

Advances Related to United States and International Mineral Resources: Developing Frameworks and Exploration Technologies

Edited by RICHARD W. SCOTT, JR., PAMELA S. DETRA, *and* BYRON R. BERGER

U.S. GEOLOGICAL SURVEY BULLETIN 2039

*The Bulletin reports some accomplishments of the
U.S. Geological Survey in research on
mineral resources in 1992*



UNITED STATES GOVERNMENT PRINTING OFFICE WASHINGTON : 1993

Complete volume in USGS Pubs drawers